

Exact Coupling Threshold for Structural Transition in Interconnected Networks

Faryad Darabi Sahneh,^{1,*} Caterina Scoglio,¹ and Piet Van Mieghem²

¹Electrical and Computer Engineering Department, Kansas State University

²Faculty of Electrical Engineering, Mathematics, and Computer Science,
Delft University of Technology, Delft, The Netherlands

Interconnected networks are mathematical representation of systems where two or more simple networks are coupled to each other. Depending on the coupling weight between the two components, the interconnected network can function in two regimes: one where the two networks are structurally distinguishable, and one where they are not. The coupling threshold—denoting this structural transition—is one of the most crucial concepts in interconnected networks. Yet, current information about the coupling threshold is limited. This letter presents an analytical expression for the exact value of the coupling threshold and outlines network interrelation implications.

Most natural and human-made networks are not isolated and have external interactions. Interconnected networks are mathematical representation of systems where two or more simple networks are coupled to each other. The importance and challenges of these networks have recently attracted substantial attention in network science. In particular, researches have addressed several fundamental problems on dynamical processes over interconnected networks such as percolation [1, 2], epidemic spreading [3–5], and diffusion [6]. These networks exhibit properties such as synchronizability [7], communicability [8], navigability [9], very different from isolated networks.

Among the most relevant dynamics on networks is the diffusion dynamics. Hernandez et al. [10] studied the full spectrum of interconnected networks where the component networks are identical. Using perturbation techniques, Gomez et al. [6] studied the diffusion dynamics on interconnected network of two non-identical networks for weak coupling as well as strong coupling. Significantly, they identified superdiffusivity, where diffusion in the interconnected network occurs faster than each network individually. Sole-Ribalta et al. [11] studied the general case, where more than two networks are interconnected with arbitrary one-to-one correspondence structure. Radicchi and Arenas [12] identified a structural transition point depending on the coupling weight between two networks: the collective interconnected network can function in two regimes, one where the two networks are structurally distinguishable and one where they are not. In a similar context, D’Agostino [13] showed adding intralinks between networks causes the structural transition from intermode to intramode. For a class of random network models according to intralayer and interlayer degree distribution, Radicchi [14] showed when correlation between intralayer and interlayer degrees is below a threshold value, the interconnected networks become indistinguishable.

Consider an interconnected network \mathbf{G} , consisting of two networks G_A and G_B , each of size N , with one-to-one interconnection with coupling weight $p > 0$, as depicted in Figure 1. Let matrices A and B represent adjacency matrices of G_A and G_B , respectively. The overall adjacency

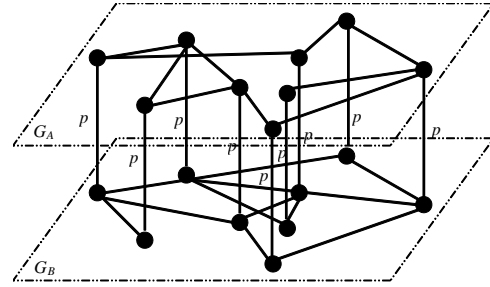


FIG. 1: One-to-one interconnection of two networks G_A and G_B , where the interconnection weight is $p > 0$.

matrix and Laplacian matrix [15] of the interconnected network \mathbf{G} are

$$\mathbf{A} = \begin{bmatrix} A & pI \\ pI & B \end{bmatrix}, \quad \mathbf{L} = \begin{bmatrix} L_A + pI & -pI \\ -pI & L_B + pI \end{bmatrix},$$

where L_A and L_B are the Laplacian matrices of G_A and G_B , respectively, and I is the identity matrix.

We denote the eigenvalues of the Laplacian matrix \mathbf{L} by $0 = \lambda_1 < \lambda_2 \leq \dots \leq \lambda_{2N}$ which satisfy the following equation

$$\begin{bmatrix} L_A + pI & -pI \\ -pI & L_B + pI \end{bmatrix} \begin{bmatrix} V_A \\ V_B \end{bmatrix} = \lambda \begin{bmatrix} V_A \\ V_B \end{bmatrix}, \quad (1)$$

where V_A and V_B contain elements of the eigenvector corresponding to G_A and G_B , respectively, and satisfy the following eigenvector normalization

$$V_A^T V_A + V_B^T V_B = 2N. \quad (2)$$

For the Laplacian matrix \mathbf{L} , $\lambda_1 = 0$ and the corresponding eigenvector is $V_A = V_B = u \triangleq [1, \dots, 1]^T$. The algebraic connectivity of the interconnected network is the smallest positive eigenvalue of the Laplacian matrix \mathbf{L} , which we represent by $\lambda_2(\mathbf{L})$. Interestingly, $\lambda = 2p$ and $V_A = -V_B = u$ is always a solution to the eigenvalue problem (1). Therefore, if p is small enough, the algebraic connectivity of the interconnected network is $\lambda_2 = 2p$. The eigenvector corresponding to $\lambda_2 = 2p$, i.e., $V_A = -V_B = u$, indicates that networks G_A and G_B

are structurally distinct. By increasing the coupling weight p , this eigenvalue may no longer be the second smallest one. Recently, Radicchi and Arenas [12] argued that there exists a threshold value p^* , so that $\lambda_2 = 2p$ no longer is the algebraic connectivity for $p > p^*$. This transition is an important phenomena as it indicates an abrupt transition in structure of the interconnected network [12]: *when $p < p^*$, the two networks are distinct while for coupling weight larger than the threshold, the overall interconnected network functions as a single network.* In other words, for $p > p^*$, the two networks are not structurally distinguishable.

Gomez et al. [6] showed that the algebraic connectivity of \mathbf{L} is upper-bounded by the half of the algebraic connectivity of the superpositioned network G_s with adjacency matrix $A + B$, i.e., $\lambda_2(\mathbf{L}) \leq \frac{1}{2}\lambda_2(L_A + L_B)$. This upper-bound is true for any value of the coupling weight p , and becomes exact as $p \rightarrow \infty$. Using this result, Radicchi and Arenas [12] argued that the coupling threshold is upper-bounded by one fourth of the algebraic connectivity of the super-positioned network, which is equivalent to

$$p^* \leq \frac{1}{2}\lambda_2\left(\frac{L_A + L_B}{2}\right). \quad (3)$$

Although the coupling threshold p^* is a critical quantity for interconnected networks, little is known apart from the upper-bound (3). In this Letter, we *derive the exact value of the coupling threshold p^** and present tight bounds that we interpret physically.

We first need to understand how the eigenvalues of \mathbf{L} vary with p . Since the elements of the Laplacian matrix \mathbf{L} are continuous functions of p , so are the eigenvalues of \mathbf{L} [16]. This implies that the transition in the algebraic connectivity of the interconnected network is not a result of any abrupt transitions of the eigenvalues of \mathbf{L} , but rather due to crossing of eigenvalues trajectories as function of p . Specifically, the algebraic connectivity transition occurs precisely at the point where the second and third eigenvalues of \mathbf{L} coincide. Therefore, *the coupling threshold p^* is such that $2p^*$ is a repeated eigenvalue of \mathbf{L} .*

Our approach to find the exact value of p^* is through eigenvalue sensitivity analysis. The key idea is that while a first-order differentiation of eigenvalues simply determines eigenvalue/eigenvector sensitivity for discrete eigenvalues [17], this method cannot uniquely find the eigen-derivatives for repeated eigenvalues [18]. Hence, we study the system of equations for eigenvalue and eigenvector derivatives with respect to p , which we refer to as eigen-derivatives, at $\lambda = 2p$, and look for critical value of p^* such that a unique solution does not exist. This Letter includes the main results and procedures of our mathematical deductions, while further details are available in the Supplemental Material [19]. Differentiating (1) and (2) with respect to p yields the governing equations for the eigen-

derivatives $\frac{dV_A}{dp}$, $\frac{dV_B}{dp}$, and $\frac{d\lambda}{dp}$ at $\lambda = 2p$

$$\begin{bmatrix} L_A - pI & -pI & -u \\ -pI & L_B - pI & u \\ -u^T & u^T & 0 \end{bmatrix} \begin{bmatrix} \frac{dV_A}{dp} \\ \frac{dV_B}{dp} \\ \frac{d\lambda}{dp} \end{bmatrix} = \begin{bmatrix} -2u \\ 2u \\ 0 \end{bmatrix}. \quad (4)$$

As expected, for $\lambda = 2p$ and $V_A = -V_B = u$, $\frac{dV_A}{dp} = \frac{dV_B}{dp} = 0$ and $\frac{d\lambda}{dp} = 2$ always satisfy Eq. (4). However, the key idea is that when $\lambda = 2p$ is a repetitive eigenvalue, the eigen-derivative equation (4) does not have a unique solution. This occurs when the matrix

$$W \triangleq \begin{bmatrix} L_A - pI & -pI & -u \\ -pI & L_B - pI & u \\ -u^T & u^T & 0 \end{bmatrix} \quad (5)$$

is singular. As shown in [19], W is singular for $p^* = \frac{1}{2}\lambda_i(Q)$ where the $N \times N$ matrix Q is defined as $Q \triangleq \bar{L} - \tilde{L}\tilde{L}^\dagger\tilde{L}$, and \bar{L} and \tilde{L} are

$$\bar{L} \triangleq \frac{L_A + L_B}{2}, \quad \tilde{L} \triangleq \frac{L_A - L_B}{2}, \quad (6)$$

and † superscript denotes the Moore–Penrose pseudo-inverse [15]. Therefore, repeated eigenvalues occur at $\lambda = 2p^*$ for the values of $p^* = \frac{1}{2}\lambda_i(Q)$, for $i \in \{1, \dots, N\}$. This indicates that repeated eigenvalues can occur for N different values of p^* . For the transition in algebraic connectivity, the coupling threshold is the smallest positive solution. Therefore, the exact coupling threshold is

$$p^* = \frac{1}{2}\lambda_2(Q) \quad (7)$$

Since term $\tilde{L}\tilde{L}^\dagger\tilde{L}$ in Q is a positive semi-definite matrix, $p^* = \frac{1}{2}\lambda_2(Q) = \frac{1}{2}\lambda_2(\bar{L} - \tilde{L}\tilde{L}^\dagger\tilde{L}) \leq \frac{1}{2}\lambda_2(\bar{L})$ which confirms the upper-bound (3) in [12]. Interestingly, the exact value not only depends on \bar{L} , half of the Laplacian of the superpositioned network, it also depends on \tilde{L} , which corresponds to the difference between networks G_A and G_B . After some algebraic manipulations (see [19]), Q can be alternatively expressed as

$$Q \triangleq \bar{L} - \tilde{L}\tilde{L}^\dagger\tilde{L} \quad (8)$$

$$= 2(L_A - \frac{1}{2}L_A\bar{L}^\dagger L_A) = 2(L_B - \frac{1}{2}L_B\bar{L}^\dagger L_B) \quad (9)$$

$$= L_A\bar{L}^\dagger L_B = L_B\bar{L}^\dagger L_A \quad (10)$$

Furthermore, according to (7) and (10), the coupling threshold p^* can be alternatively obtained as

$$p^* = \frac{1}{\rho(L_A^\dagger + L_B^\dagger)}, \quad (11)$$

where $\rho(\bullet) \triangleq \lambda_N(\bullet)$ denotes spectral radius (see [19]). Finally, expressions (8), (9), and (10) for Q provide upper-bound and lower bound for the coupling threshold $p^* =$

$\frac{1}{2}\lambda_2(Q)$ in terms of the spectral radius of each isolated network G_A and G_B , as well as the super-positioned network G_s as

$$p^* \geq \frac{1}{\lambda_2^{-1}(L_A) + \lambda_2^{-1}(L_B)}, \quad (12)$$

$$p^* \leq \min\{\lambda_2(L_A), \lambda_2(L_B), \frac{1}{2}\lambda_2(\bar{L})\}. \quad (13)$$

The lower-bound (12) has a very elegant expression, as it is half of the *harmonic mean* of $\lambda_2(L_A)$ and $\lambda_2(L_B)$. The upper-bounds (13) not only includes the upper-bound $\frac{1}{2}\lambda_2(\bar{L})$, reported in [12], but also it indicates a fundamental property of interconnected networks: the coupling threshold p^* is upper-bounded by the algebraic connectivity of the least-connected network. Furthermore, if the algebraic connectivity of one network is at least three times smaller than that of the other network, i.e., $\lambda_2(L_A) < \frac{1}{3}\lambda_2(L_B)$ without loss of generality, then the algebraic connectivity of the least-connected network, here G_A , mainly determines the coupling threshold, and the super-positioned network does not play a major role. Indeed, if $K \triangleq \lambda_2(L_B)/\lambda_2(L_A) > 3$, then

$$\frac{K}{1+K}\lambda_2(L_A) < p^* \leq \lambda_2(L_A). \quad (14)$$

While the upper-bounds and lower-bound (12) and (13) are simple, they do not include much information regarding interrelations of network components. We can find bounds that explicitly depend on the networks interrelations. We can use formula (11) to build an upper-bound $p^* \leq \frac{1}{\hat{\rho}_{n_A, n_B}}$ using the eigenvectors corresponding to the n_A smallest positive eigenvalue of L_A and the n_B smallest positive eigenvalue of L_B [19], where $\hat{\rho}_{n_A, n_B}$ is the spectral radius of an $(n_A + n_B)$ -by- $(n_A + n_B)$ matrix, i.e.,

$$\hat{\rho}_{n_A, n_B} = \rho \left(u_{(n_A+n_B)} \begin{bmatrix} \lambda^{-1}(L_A) \\ \lambda^{-1}(L_B) \end{bmatrix}^T \circ \begin{bmatrix} I_{n_A} & \mathbf{v}_A^T \mathbf{v}_B \\ \mathbf{v}_B^T \mathbf{v}_A & I_{n_B} \end{bmatrix} \right), \quad (15)$$

where, \circ denotes the Hadamard (entry-wise) product, $\lambda^{-1}(L_A) \triangleq [\lambda_2^{-1}(L_A), \dots, \lambda_{n_A+1}^{-1}(L_A)]^T$, $\mathbf{v}_A = [v_2(L_A), \dots, v_{n_A+1}(L_A)] \in \mathbb{R}^{N \times n_A}$, and $\lambda^{-1}(L_B)$ and \mathbf{v}_B are defined similarly. The interesting aspect of this upper-bound is that it not only depends on the smallest positive eigenvalues of L_A and L_B , it also depends on the inner-product of their corresponding eigenvectors, thus explicitly incorporating networks interrelation. By computing a few eigenvectors of L_A and L_B , this upper-bound gives very good estimates, with increasing precision as the number of eigenvectors n_A and n_B increases.

In the following, we perform several numerical simulations to investigate our analytical results. First, we generate an interconnected network with $N = 1000$, where graph G_A is a scale-free network with exponent $\gamma = 3$, and G_B is a random geometric network with threshold distance $r_c = \sqrt{\frac{5 \log N}{\pi N}}$. For these networks, $\lambda_2(L_A) = 0.355$, and

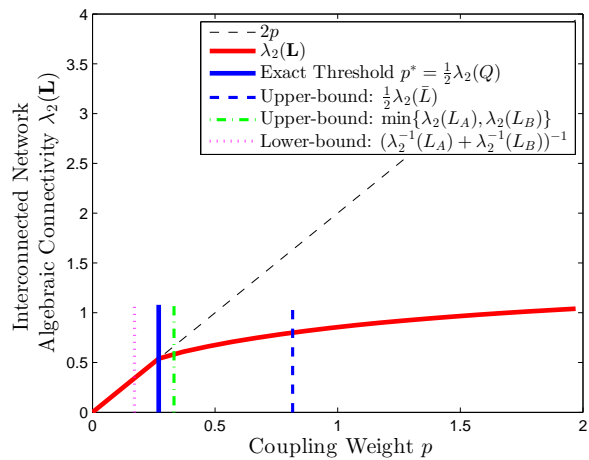


FIG. 2: Algebraic connectivity $\lambda_2(L)$ of two coupled networks as a function of the coupling weight p . For $p < p^* = 0.27$, algebraic connectivity is $\lambda_2(L) = 2p$. For $p > p^*$, eigenvalue $\lambda = 2p$ is no longer the algebraic connectivity of the interconnected network; thus, denoting a structural transition at $p = p^*$.

$\lambda_2(L_B) = 0.332$. Figure 2 shows the algebraic connectivity $\lambda_2(L)$ of the interconnected network as a function of the coupling weight p , and illustrates that formula (7) predicts the coupling threshold exactly. Furthermore, this simulation supports the analytical results for bounds in (13) and (12). In order to highlight different aspects of topological properties of interconnected networks, we design two numerical experiments: one for a set of interconnected networks \mathbf{G} with identical superpositioned network G_s , and one for a set of interconnected networks \mathbf{G} with isomorphic network components G_A and G_B .

For the first set of interconnected networks with identical superpositioned network, we generate a set of interconnected networks from the Karate Club network according to the following rule: $a_{ij} = a_{ji} = p_{ij}w_{ij}$ and $b_{ij} = b_{ji} = (1 - p_{ij})w_{ij}$ for $j < i$, where w_{ij} 's are the elements of the weighted Karate Club adjacency matrix and p_{ij} 's are i.i.d. uniformly distributed on $[0, 1]$. In this way, the super-positioned network will always be the same for any realization of this interconnected network generation. Therefore, differences in the outputs do not depend on the superpositioned network. Figure 3 shows different bounds for the coupling threshold versus the exact values. The upper-bound $\frac{1}{2}\lambda_2(\bar{L})$ is the same even though the exact threshold p^* has a broad distribution. When p^* is small, the upper-bound $\min\{\lambda_2(A), \lambda_2(B)\}$ is accurate, i.e. close to, but above the $y = x$ line (black dashed line). This region represents interdependent networks where one network component is loosely connected and possesses a relatively small algebraic connectivity. As discussed in (14), in these cases the value of the coupling threshold is mainly determined by the algebraic connectivity of the least connected network, which explains why $\min\{\lambda_2(A), \lambda_2(B)\}$ leads to accurate predictions.

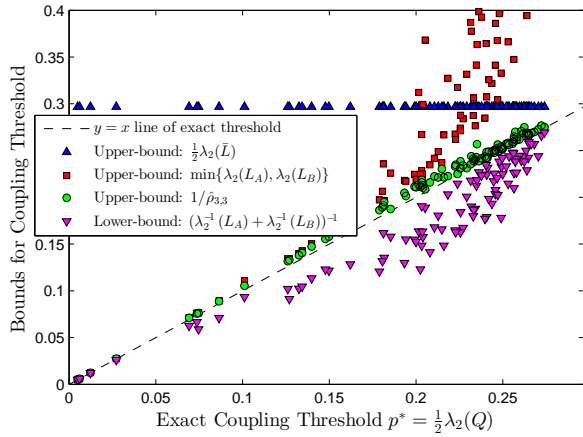


FIG. 3: Bounds for the coupling threshold versus the exact values for a set of interconnected networks with identical averaged network. Specifically, weighted networks G_A and G_B are randomly generated such that $A + B$ is the adjacency matrix of the weighted Karate Club network. For each generated network, we compute different bounds for the coupling threshold and compare them with the exact value. The closer to the black dashed line, the more accurate the bounds.

For the second set of interconnected networks with isomorphic network components G_A and G_B , we generate another set of interconnected networks for which we use the adjacency matrix of the Karate club network as A , and then pick the adjacency matrix of G_B as $B = P^{-1}AP$, where P is a randomly chosen permutation matrix. In this way, G_B is basically the Karate Club network, however, with different node labels. Therefore, G_A and G_B are isomorphic and have identical graph properties. Therefore, different outputs are purely due to the interrelation between G_A and G_B . For each generation of such interconnected network, Figure 4 shows several bounds for the coupling threshold plotted versus the exact value. Note that the upper-bound $\min\{\lambda_2(A), \lambda_2(B)\}$ and lower-bound $(\lambda_2^{-1}(A) + \lambda_2^{-1}(B))^{-1}$ are always constant, as these values only depend on the graph properties of G_A and G_B , which are kept identical. There is a significant negative correlation between the coupling threshold and Fiedler vectors of G_A and G_B (i.e., $|v_2^T(L_A)v_2(L_B)|$). The coupling threshold is maximal when the two networks are uncorrelated (i.e., $|v_2^T(L_A)v_2(L_B)| \rightarrow 0$) and decreases as the two networks become more correlated ($|v_2^T(L_A)v_2(L_B)| \rightarrow 1$). We remark that here the correlation between G_A and G_B is measured in terms of their Fiedler vectors, and that other correlation metrics—such as degree correlation—do not necessarily yield similar results. See, [19] for further information.

In conclusion, this Letter computes exactly the critical value p^* for the coupling weight in an interconnected network G , for which only a few bounds were known so far. The exact expression of the coupling threshold p^* not only depends on individual network components G_A and G_B

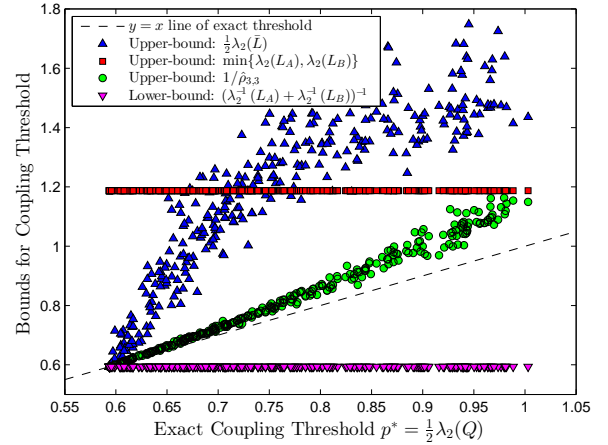


FIG. 4: Bounds for the coupling threshold versus the exact values for a set of interconnected networks where network G_A and G_B are isomorphic and thus have identical graph properties. For each generated network, we compute different bounds for the coupling threshold and compare them with the exact value. The closer to the black dashed line, the more accurate the bounds.

or the superpositioned network G_s , but also depends on the interrelation of G_A and G_B . Yet, it is possible to detect upper and lower bounds for the coupling threshold p^* only in terms graph properties of G_A , G_B , and G_s . These types of bounds are important, even though they lack a description of the interconnection relation between G_A and G_B . The exact expression for p^* directly led to new upper and lower bounds only in terms of graph properties of G_A , G_B , and G_s . Furthermore, we developed the upper-bound (15) with tunable accuracy, which explicitly depends on the network interrelation. Through analytic arguments and a specific design of numerical experiments, we showed that the superpositioned network G_s is physically irrelevant for the identification of the coupling threshold when one of the network components is considerably less connected, or when the network components G_A and G_B are uncorrelated according to their Fiedler eigenvectors inner product, i.e., when $|v_2^T(L_A)v_2(L_B)|$ is small. Even though the analysis has been performed for coupling of two networks, we expect the methodology to be generalizable to multiple coupled networks, as p^* is the critical value for the coupling weight p for which the eigen-derivative equations do not have unique solutions. Hence, this Letter sheds new light on the true nature of structural transitions in interconnected networks, outlining the importance of topological interrelations in such networks.

Acknowledgement. We would like to thank Filippo Radicchi and Alex Arenas for their helpful suggestions to improve this manuscript. This work has been supported by the National Science Foundation Award CIF-1423411. Any findings, recommendations, and opinions in this work are those of the authors and do not necessarily reflect the views of the National Science Foundation.

-
- * Electronic address: faryad@ksu.edu
- [1] S. V. Buldyrev, R. Parshani, G. Paul, H. E. Stanley, and S. Havlin, *Nature* **464**, 1025 (2010).
- [2] Y. Hu, B. Ksherim, R. Cohen, and S. Havlin, *Phys. Rev. E* **84**, 066116 (2011).
- [3] A. Saumell-Mendiola, M. Á. Serrano, and M. Boguñá, *Phys. Rev. E* **86**, 026106 (2012).
- [4] H. Wang, Q. Li, G. D'Agostino, S. Havlin, H. E. Stanley, and P. Van Mieghem, *Phys. Rev. E* **88**, 022801 (2013).
- [5] F. Sahneh, C. Scoglio, and F. Chowdhury, in *American Control Conference (ACC)* (2013), pp. 2307–2312, ISSN 0743-1619.
- [6] S. Gómez, A. Diaz-Guilera, J. Gómez-Gardeñes, C. J. Pérez-Vicente, Y. Moreno, and A. Arenas, *Phys. Rev. Lett.* **110**, 028701 (2013).
- [7] J. Aguirre, R. Sevilla-Escoboza, R. Gutiérrez, D. Papo, and J. Buldu, *Phys. Rev. Lett.* **112**, 248701 (2014).
- [8] E. Estrada and J. Gómez-Gardeñes, *Phys. Rev. E* **89**, 042819 (2014).
- [9] M. De Domenico, A. Solé-Ribalta, S. Gómez, and A. Arenas, *Proc. Natl. Acad. Sci.* p. 201318469 (2014).
- [10] J. Martín-Hernández, H. Wang, P. Van Mieghem, and G. D'Agostino, *Physica A* **404**, 92 (2014).
- [11] A. Solé-Ribalta, M. De Domenico, N. E. Kouvaris, A. Díaz-Guilera, S. Gómez, and A. Arenas, *Phys. Rev. E* **88**, 032807 (2013).
- [12] F. Radicchi and A. Arenas, *Nat. Phys.* **9**, 717 (2013).
- [13] G. D'Agostino, in *Nonlinear Phenomena in Complex Systems: From Nano to Macro Scale* (Springer, 2014), pp. 111–131.
- [14] F. Radicchi, *Phys. Rev. X* **4**, 021014 (2014).
- [15] P. Van Mieghem, *Graph Spectra for Complex Networks* (Cambridge Univ Pr, 2011).
- [16] M. Zedek, *Proc. Amer. Math. Soc.*, Proc. **16**, 78 (1965).
- [17] R. B. Nelson, *AIAA journal* **14**, 1201 (1976).
- [18] W. C. Mills-Curran, *AIAA journal* **26**, 867 (1988).
- [19] F. D. Sahneh, C. Scoglio, and P. Van Mieghem, *Supplemental Material* (2014).